

# CATALYST ENHANCED MICRO SCALE BATCH ASSEMBLY

Rajashree Baskaran<sup>1,2</sup>, Ji Hao Hoo<sup>1</sup>, Bowen Cheng<sup>1</sup>, Karl F Böhlinger<sup>1</sup>

<sup>1</sup>Department of Electrical Engineering, University of Washington, Seattle, USA

<sup>2</sup>Components Research, Intel Corporation, USA

## ABSTRACT

We enhance the efficiency of assembly of microparts in batch dry assembly methods studied previously by our group. Here we study the system dynamics with the addition of a few non-participating millimeter scale parts that act as ‘catalysts’. We present experimental results that show 25-50% reduction in acceleration needed to trigger part motion and up to 4 times increase in concentration of parts in motion due to addition of catalysts. We adapt a model from chemical kinetic theory to understand our system behavior.

## 1. INTRODUCTION TO MICROSCALE ASSEMBLY

Many parallel assembly processes in the microscale have been studied previously. These include use of liquid flow to deliver parts that fall into traps [1], use of surface tension of liquids in predefined locations for part capture including various polymers [2] and solders [3]. We have studied fully dry assembly methods in vibratory platforms in the micro scale [4-6]. For materials that may be sensitive to exposure to water or other liquid environments, these all-dry assembly methods offer a feasible alternative to fluidic parallel assembly.

Batch assembly using vibration is a cost effective and fast alternative to pick-and-place robotics. In this assembly process, microparts are assembled into microfabricated deep trenches using acoustic vibration. The vibration acceleration ( $G$ ) supplied should be high enough to keep the parts in motion but lower than a critical threshold to keep the assembled parts in their traps. Hence for optimal assembly, the microparts should be set in motion at low vibration (typically  $<10g$ ). For part lateral size  $<1mm$  and thickness  $<500\mu m$  van der Waals forces are at least an order of magnitude stronger than gravity for silicon parts and highly dependent on ambient conditions (humidity and temperature).

## 2. MODEL DEVELOPMENT

Modeling of microscale assembly processes using a chemical reaction analogy was introduced in [7]. The chemical analogy to our system is explained in Fig. 1 and Table 1. We define 3 states for the parts, A when the parts are outside of the assembly sites (initial state),  $A^*$  when the parts are in free motion (activated) and B when the parts are assembled onto the assembly sites (final desired state). The activation energy can be thought of as the height of the potential barrier that is separating two minima of potential energy (of the reactants and of the products of reaction). In our case, the van der Waals and other surface forces are the source of this ‘energy barrier’.

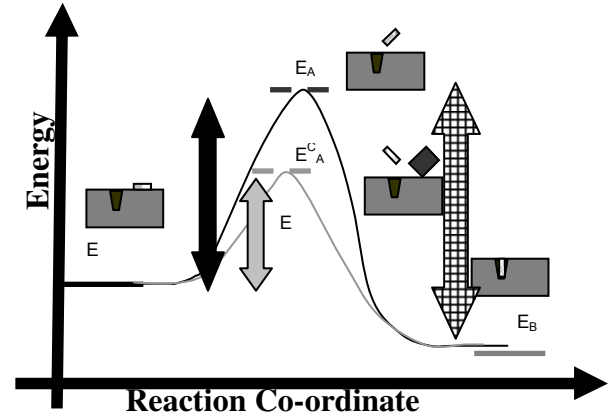


Fig. 1: Schematic showing the energy states for the assembly process  $A \rightarrow B$ . The black arrow represents the energy barrier without catalyst and the grey with catalyst. The checkered arrow shows the energy required for the reverse reaction  $B \rightarrow A$ .

| Chemical reaction                 | Reactant                        | Products                        | Activated Reactant           | Energy Barrier      | Temperature        |
|-----------------------------------|---------------------------------|---------------------------------|------------------------------|---------------------|--------------------|
| $A \rightarrow A^* \rightarrow B$ | A                               | B                               | $A^*$                        | $E$                 | $T$ or $G$         |
| <b>Micropart dry assembly</b>     | parts outside the assembly site | parts inside the assembly traps | parts in air (parts jumping) | van der Waals force | stage acceleration |

Table 1: Variables in the model of the batch assembly process that is developed in analogy to chemical reaction kinetics. Note that for the stage acceleration  $G$  and sinusoidal displacement  $x$  with frequency  $f$ ,  $G = (2\pi f)^2 x$ .

A catalyst functions by lowering the energy barrier of the reaction. In our dry assembly set up, parts whose van der Waals force to inertial force ratio is small can be triggered to move with smaller external acceleration. Once there is motion within the assembly box, many parts are triggered to move. We use this principle to pick a catalyst that is  $2mm \times 2mm \times 0.5mm$ , whereas our parts are  $800\mu m \times 800\mu m \times 50\mu m$ .

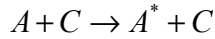
Another notion that is important to understand in this context is that of concentration of reactants (total number of parts in a given surface area). In our particular case, the behavior of the parts under external agitation is also dependent on the concentration. When there is an overlap or adhesion between two parts at the initial state, the effective van der Waals force of the combined part is different from that of the individual parts. As the density of the parts

increases, the likelihood of part overlap is high and their combined van der Waals force induced barrier is lower. Also, once one or a few parts start moving, they trigger other parts into motion; hence the barrier is a function of the distribution of individual part on the surface and part-part interactions.

Typical dynamics of chemical reactions are modeled by differential equations that relate the rate of product formation and reactant consumption to concentrations of the reactants and products, and intermediate species. Note that for the case of systems with catalysts, the concentration of such catalyst species is also required to capture the correct dynamics. A typical reaction dynamics is written as the following equation where  $X$  and  $Y$  are the different reactant species.

$$\text{Rate} \equiv -\frac{d[X]}{dt} = \kappa[X]^m[Y]^n \quad (1)$$

The order of a reaction is defined as the sum of the powers  $m$  and  $n$  in equation 1. The order for a chemical system with respect to each reactant is experimentally determined, which can be integer or non-integer, typically a value between -2 to 3. The negative values denote species that actively inhibit product formation. The proportionality constant  $\kappa$  is called the rate coefficient and is independent of the concentration. For many elementary reactions, the number of reactants that are involved in a reaction step is also the order of the reaction. For reactions with catalytic activity, the concentration of the catalyst also affects the reaction rate. In our micro scale system, it is difficult to estimate the overall order of our reaction. There are many elementary steps involved in the assembly process. All the possible elementary steps that were observed in our experiments for part activation are represented in equation 2, where  $C$  is the catalyst. Even in the absence of catalysts, our system behaves in an autocatalytic fashion, i.e., an activated part ‘hits’ a stuck part and activates it.



The rate coefficient is typically a strong function of the temperature at which the reaction is occurring. In chemical reaction kinetics, the Arrhenius equation (Equation 3) states that the reaction rate coefficient  $\kappa$  depends on the ratio of activation energy  $\Delta E$  and  $RT$ , where  $R$  is the gas constant and  $T$  the temperature. This implies that either an increase in  $G$  (our system ‘ $T$ ’) or addition of catalysts, which reduces the energy barrier  $\Delta E$ , must have the same effect of increasing  $\kappa$ .

$$\kappa \propto e^{\frac{-\Delta E}{RT}} \quad (3)$$

In this study, we present experimental measurements of the energy barrier with and without catalysts. We also present experimental data on the rate at which parts are

activated for the case of different reaction ‘temperatures’. This rate of formation of  $A^*$  is directly dependent on the rate coefficient. The exact relationship of this dependence is a function of the order.

### 3. EXPERIMENTAL DETAILS

The experimental set-up and flow of data is shown in Figure 2. The parts ( $800 \times 800 \times 50 \mu\text{m}^3$ ) and catalysts ( $2 \times 2 \times .5 \text{mm}^3$ ) are made respectively from SOI/silicon wafers using standard lithography and DRIE etching. A polished silicon wafer is used as the assembly surface. For enabling close observation of the part motion due to vibration of the acoustic actuator, we confine the parts using an optically transparent container. A high speed camera is mounted to view the part motion with high intensity backlighting that makes the parts appear dark in strong contrast to the light background.

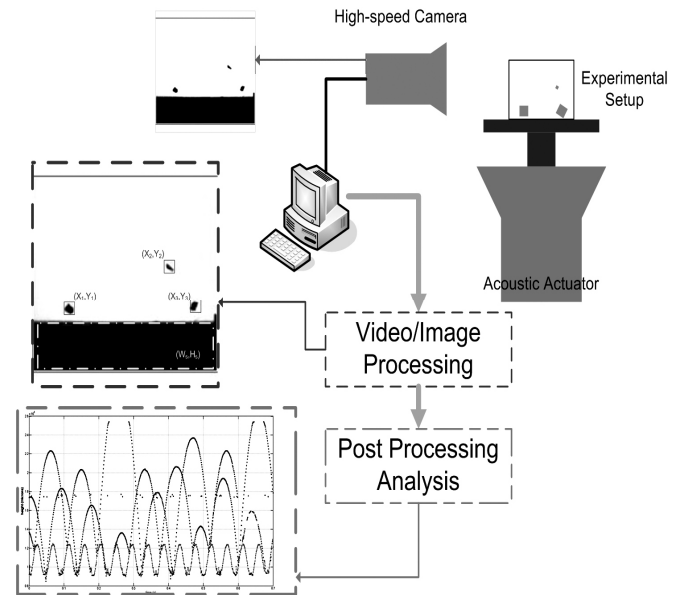


Fig. 2: Schematic of the experimental set-up: An assembly box (2.5cm wide, 10cm tall and 2.5mm deep) confines the part on a microfabricated substrate which is vibrated vertically using a LabView© controlled function generator. The high speed camera images are processed and analyzed using Matlab©.

Dedicated Matlab© routines were developed for image processing and subsequent data reduction. Typically, we extract the vertical and horizontal position of the center of mass of the parts from the sideview videos as a function of time. The stage motion is also tracked as a function of time. The lower left frame in Figure 2 shows the sinusoidal motion of the stage and the corresponding vertical motion (note the parabolic paths) of two parts. Figure 3 shows the center of mass position (both in-plane and vertical) vs. time for two parts. Note that while the vertical trajectories of the part are parabolas (governed mainly by gravity), the horizontal trajectories are governed by the mechanics of part-substrate interaction at each ‘collision,’ which is complicated for a cuboid part that could have edge or side impacts.

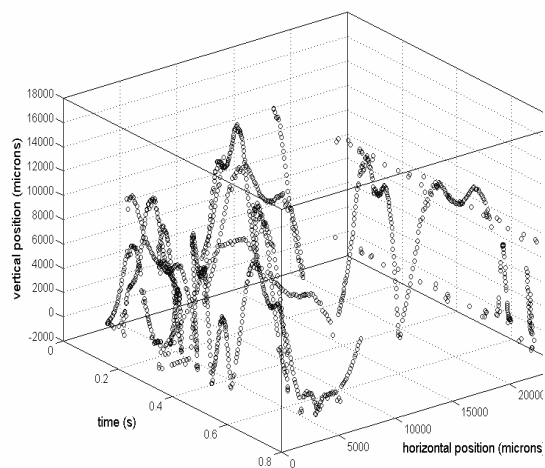


Fig. 3: A typical output from the image processing system. In this case, we plot the path of two parts moving in the box where the part motion is confined to one dimension in the plane of the substrate (depth 2.5mm). We plot here the vertical and horizontal positions of the part as a function of time from a video taken at 800 frames per second.

Since the part motion dynamics happens in a time scale of milliseconds, the high speed video recording and the subsequent image analysis is an important tool for understanding the mechanism of part motion. For instance, Figure 4 shows data from a video segment that tracks part motion initiated in a case without catalysts, when 2 partially overlapping or ‘stuck’ parts are initially triggered to joint motion ( $\sim 8.12$ s) that then separate into 2 parts after the second impact with the stage ( $\sim 8.25$ s, indicated by an arrow in the figure).

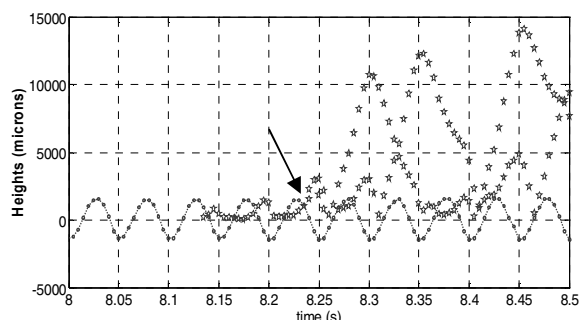


Fig. 4: The vertical position of the stage (dashed) and center of mass of 2 parts (stars) that are initially ‘stuck’ (appear as 1 part) from image processing of a high speed video.

#### 4. RESULTS AND DISCUSSION

We perform a set of experiments to measure the energy barrier of our parts for different concentrations of parts, which is analogous to the concentration of the reactants in a chemical reaction. We start with an assembly box with the parts with no stage motion. We then ramp the

acceleration of the stage in small steps of  $\sim 0.05g$ . We note the instantaneous acceleration where the part starts to ‘jump’ and denote this as the minimum  $G$  required to initiate part motion.

Figure 5 shows the minimum  $G$  required to initiate formation of  $A^*$  with and without catalysts for various initial part concentrations. Note that there is little difference between additions of 1 or 3 catalysts. Also note that the standard deviation from the 5 experiments is very small for the case with the catalysts, compared to that without. These data also show that the presence of a catalyst is essential for any part motion below  $10g$  acceleration for low concentrations of parts.

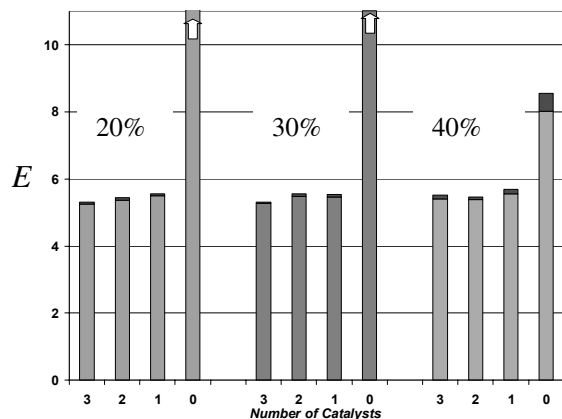


Fig. 5: Energy barrier to formation of  $A^*$  from A: Minimum acceleration of the stage (non-dimensionalized to acceleration due to gravity) at which parts start to jump. The values are averaged from 5 experiments with the standard deviation in black. For 20% and 30% part densities, the acceleration required to move the parts were larger than  $10g$  and highly distributed. On addition of a catalyst, micropart motion was consistently triggered at less than  $6g$ .

Our next set of experiments was aimed at measuring the rate of formation of  $A^*$  by addition of a catalyst at various ‘temperatures’ of our system. From the chemical reaction analogy, we expect from the Arrhenius equation that the addition of a catalyst must have the same effect on reaction coefficient as operating at a higher acceleration of the stage.

In order to measure the rates in which the parts were getting activated, we recorded videos starting at low stage acceleration (from  $5g$ ), below the threshold for part motion. We increased the acceleration to various final values in one time step. From the image processing of the videos, we gather the data on individual part locations as a function of time. From this information, we can extract the data on total number of parts that are jumping (center of mass above a critical threshold value). In this plot, the real time axis is shifted such that  $t=0$  is the frame before the first frame at which at least one part jumped. All the videos were taken at the same frame rate of 1000 frames per second. Figure 6 shows the initial reaction rate for the case of  $G=10.6g$  with and without addition of catalyst. As expected, the reaction rate increases ( $\sim 3\times$ ) in the presence of catalysts.

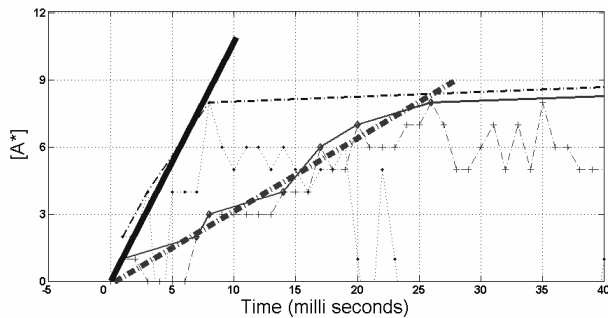


Fig.6: Initial rates of formation of  $A^*$  with and without catalyst for the case of 10.6g. Note the very fast initial rates (1000#/s and 300#/s). The time it takes for half of steady state  $A^*$  to form,  $t_{1/2}$ , is  $\sim 0.01$  s and  $\sim 0.02$ s with and without catalyst, respectively.

To measure the effect of a catalyst on the assembly process, we studied its influence on assembly rates in comparison with an increase of the stage acceleration. If the parts can be activated using catalysts instead of using higher stage acceleration, assembly can be achieved at lower ‘temperature’ of the system. This is a vital aspect of the assembly process as this would potentially enable good assembly yields since we can operate at energies below the level at which the parts will be triggered out of the traps.

Figure 7 shows experimental results of the rates of formation of  $A^*$  at different  $G$  values. As the  $G$  values increase from 9g to 12.7g, without catalysts, the total number of activated parts increases from 3 to 23. In this case, the total number of parts in the assembly box was 30. But with the addition of 3 catalysts, the total number of parts in air for the case of 9g was increased 5 fold. At higher accelerations however, there is diminishing return on addition of catalysts. At 12.7 g, there is no noticeable increase in total number of parts in air.

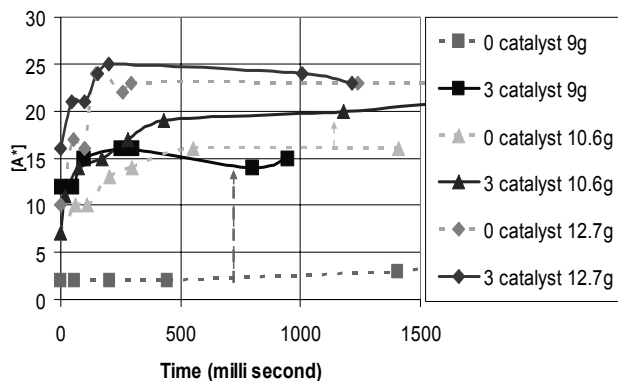


Fig. 7: Experimental measurement of concentration of parts in air  $A^*$  with catalyst (solid) and without catalyst (dashed) for the case of 30% part concentration, in this case 30 parts for various  $G$ . Note that the maximum benefit from catalyst addition is at low  $G$ . Time scale was reset at zero at the onset of part motion for all cases.

## 4. CONCLUSION AND FUTURE WORK

We present experimental evidence to support a new concept of catalyst enhanced microscale assembly. The method could offer pathways for development and realization of an efficient, economical alternative to pick-and-place robots. We also present an analytical framework inspired from chemical kinetics that can sufficiently explain the experimental data obtained.

We are currently working on measuring the van der Waals force induced barriers for different part size from 400micron to 2mm lateral size and various thicknesses. Also, we are exploring a systematic method to synthesize the optimal geometry for the ‘catalyst’ part.

## ACKNOWLEDGEMENT

This project was supported by funding from Intel Corporation.

## REFERENCES

1. Yeh, H.-J.J. and J.S. Smith, *Fluidic Assembly for the Integration of GaAs Light-Emitting Diodes on Si Substrates*. IEEE Photonics Technology Letters, 1994. **6**(6): p. 706-708.
2. Syms, R.R.A., et al., *Surface Tension-Powered Self-Assembly of Microstructures: The State-of-the-Art*. Journal of Microelectromechanical Systems, 2003. **12**(4): p. 387-416.
3. Saeedi, E., et al., *Molten-Alloy Driven Self-Assembly for Nano and Micro Scale System Integration*. Fluid Dynamics & Materials Processing, 2007. **2**(4): p. 221-246.
4. Fang, J. and K.F. Böhringer, *Wafer Level Packaging Based on Uniquely Orienting Self-Assembly (the DUO-SPASS Processes)*. ASME/IEEE Journal of Microelectromechanical Systems, 2006. **15**(3): p. 531-540.
5. Fang, J. and K.F. Böhringer, *Parallel micro component-to-substrate assembly with controlled poses and high surface coverage*. IOP Journal of Micromechanics and Microengineering (JMM), 2006. **16**: p. 721-730.
6. Wang, K., R. Baskaran, and K.F. Böhringer. *Template Based High Packing Density Assembly for Microchip Solid State Cooling Application*. in *3rd Annual Conference on Foundations of Nanoscience: Selfassembled Architectures and Devices (FNANO)*. 2006. Snowbird, UT.
6. Hosokawa, K., I. Shimoyama, and H. Miura, *Dynamics of Self-Assembling Systems - Analogy with Chemical Kinetics*. Artificial Life, 1994. **1**(4): p. 413-427.